



HAL
open science

FREQUENCY SPECTRUM OF LASER-GENERATED ULTRASONIC WAVES

B. Betz, W. Arnold

► **To cite this version:**

B. Betz, W. Arnold. FREQUENCY SPECTRUM OF LASER-GENERATED ULTRASONIC WAVES. Journal de Physique Colloques, 1983, 44 (C6), pp.C6-61-C6-65. <10.1051/jphyscol:1983609>. <jpa-00223168>

HAL Id: jpa-00223168

<https://hal.science/jpa-00223168v1>

Submitted on 4 Feb 2008

HAL is a multi-disciplinary open access archive for the deposit and dissemination of scientific research documents, whether they are published or not. The documents may come from teaching and research institutions in France or abroad, or from public or private research centers.

L'archive ouverte pluridisciplinaire HAL, est destinée au dépôt et à la diffusion de documents scientifiques de niveau recherche, publiés ou non, émanant des établissements d'enseignement et de recherche français ou étrangers, des laboratoires publics ou privés.



HAL Authorization

FREQUENCY SPECTRUM OF LASER-GENERATED ULTRASONIC WAVES

B. Betz and W. Arnold

Fraunhofer-Institute for Non-Destructive Testing, Bldg. 37, University, 6800 Saarbrücken, F.R.G.

Résumé - Le spectre des ondes ultrasonores produites grace à l'effet thermoélastique par de courtes impulsions laser a été mesuré dans l'aluminium polycristallin et dans la ceramique Si_3N_4 . Le spectre est maximum à $1/2\pi\tau$ si la forme de l'impulsion en fonction du temps est gaussienne (2τ est la largeur de l'impulsion). Pour les fréquences inférieures à $1/2\pi\tau$ le spectre est déterminé par l'épaisseur de peau thermique et la longueur d'onde ultrasonore alors que pour les hautes fréquences il est limité par les composantes de Fourier de l'enveloppe des impulsions du laser. Les valeurs absolues des amplitudes de vibration élastique sont de l'ordre de l'Angstrom pour des intensités optiques de l'ordre de 10 MW/cm^2 .

Abstract - The frequency spectrum of ultrasonic waves generated by short laser pulses due to the thermoelastic effect has been measured in polycrystalline aluminum and in the ceramic material silicon nitride. The spectrum exhibits a maximum at $1/2\pi\tau$ if the temporal laser profile is gaussian (2τ is the pulse width). For frequencies smaller than $1/2\pi\tau$, the ratio of the thermal skin depth to the sound wavelength determines the frequency spectrum, whereas at high frequencies the spectrum is limited by the Fourier components of the laser pulse envelope. The absolute magnitudes of the sound amplitudes are of the order of Å for optical intensities of $\approx 10 \text{ MW/cm}^2$.

Because of thermal expansion a periodic heat input at a solid or liquid interface is accompanied by the generation of sound waves. This is called the thermo-elastic effect and it has first been described extensively by White /1/. Experimentally this effect has been verified by various groups /2-5/. Whereas quite large optical intensities are necessary to produce significant sound amplitudes in solids, thermo-elasticity is more effective at liquid interfaces /6-9/ mainly due to the large thermal expansion of liquids. However, for practical applications such as in non-destructive testing, the generation of sound waves in solids is of greater importance. As a heat source laser pulses or chopped electron beams are used in most cases. In order to exploit thermoelasticity efficiently, it is necessary to understand the generation mechanism on the basis of a physical model and to verify its consequences experimentally. Early experiments were restricted to show the feasibility of thermo-elastic sound generation /2,3,4/. Later on the importance of mechanically constraint or unconstraint surfaces has been demonstrated /5/. Furthermore, first experiments were carried out in which the diffraction pattern of such sound sources has been examined /10/. There is little knowledge about the frequency components of thermo-elastic sound sources although this information is necessary for practical applications. We have therefore undertaken such measurements in aluminum and in the ceramic material silicon nitride as typical representatives of good and poor thermal conductors, respectively.

The experimental set-up is shown in Fig. 1. As a laser source we used a Q-switched ruby laser. The temporal profile of the pulses were gaussian with a half-width

$\tau = 25$ ns. The laser pulse intensity impinging on the surface could be varied by inserting filters of known optical density into the optical path. We measured the power of the pulses with a calibrated photodiode. The beam with a diameter of 5 mm was not focused onto the sample. In this way we obtained optical intensities up to 300 MW/cm^2 . The laser intensity was relatively homogeneous over a width of 3 mm. This was checked by measuring the lateral profile with a small slit of $21 \mu\text{m}$ width.

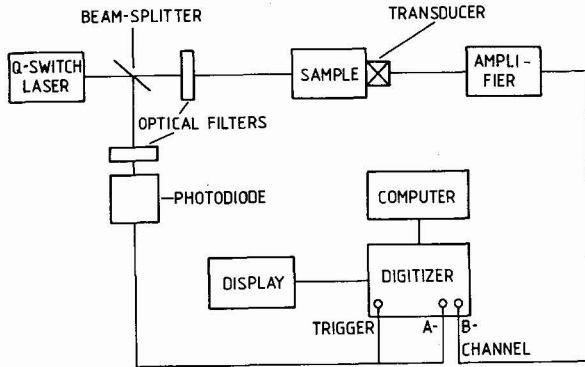


Fig.1: Schematic experimental set-up. The piezoelectric transducer has a center frequency of 60 MHz and a 6 dB bandwidth of 80 MHz.

The samples were rectangular cubes with typical dimensions of $3 \times 3 \times 3 \text{ cm}^3$. On one face of the sample a piezoelectric transducer was glued on. The receiving transducer, either sensitive to the longitudinal or transverse polarization, was always aligned along the optical axis. Its output was fed into one channel of a fast digitizer whose sample width was 5 ns. The data were then handled by a computer. In this way we obtained accurate Fourier transforms of any echo desired out of the echo sequence. A typical pulse-echo train generated in silicon nitride is shown in Fig. 2. In this case a transducer for longitudinal waves was used and the absorbed optical intensity was $\approx 50 \text{ MW/cm}^2$.

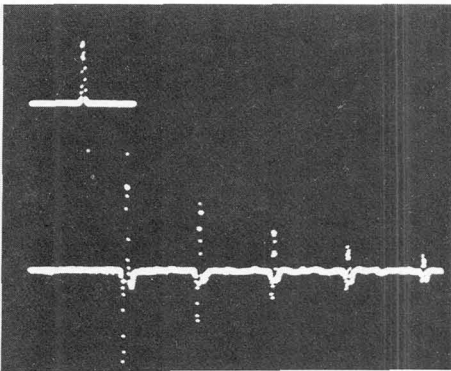


Fig.2: Pulse-echo train obtained in ceramic silicon nitride (lower trace). The predominant polarization is longitudinal. The upper trace shows the output of the photodiode, and hence represents the shape of the laser pulse.

The signal-to-noise ratio of the first echo is about 40 dB. For weaker signals the output of the transducers was first amplified by a broadband amplifier. The echo train of Fig. 2 consists mainly of longitudinal waves. The transverse polarization is suppressed at least by 25 dB even after taking into account the reduced sensitivity of the transducer for the transverse polarization. This also holds for aluminum. Figure 3 shows the frequency spectrum of the first echo in the silicon nitride sample. The spectrum was corrected by the inverse insertion loss $1/|I(\omega)|$ of the transducer and by the attenuation $\alpha(\omega)$ of the sample $/12/$. As can be seen from Fig. 3, the spectrum first increases, passes through a maximum and then

decreases rapidly. A similar behavior can be observed for all successive echoes as well as in aluminum.

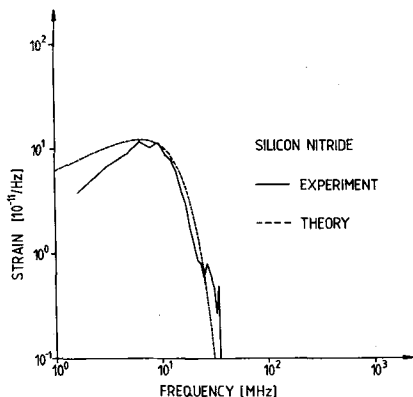


Fig.3: Frequency components of the strain pulse in silicon nitride obtained experimentally (solid line) and theoretically (dashed line). As can be clearly seen there is a maximum at $1/2\pi\tau$. The optical input power was sufficiently small so that only thermoelastic sound generation played a role.

Our experimental findings can be explained qualitatively quite simply. The thermal expansion is confined to a small layer at the surface of the sample. The extension of this layer, also called thermal skin depth, depends on the thermal properties of the material under consideration and on the frequency $\omega/2\pi$ of the periodic heat input $1/\tau$:

$$\delta = \sqrt{\frac{2\kappa}{\omega}} \quad (1)$$

Here, κ is the thermal diffusivity $\kappa = K/\rho C$, K is the thermal conductivity, ρ is the density, and C is the specific heat. Typical magnitudes of δ are $1.8 \mu\text{m}$ for silicon nitride and $4.4 \mu\text{m}$ for aluminum at $\omega/2\pi = 10^7$ Hz. This is much smaller than the corresponding sound wavelengths λ . Thus the situation is similar to driving piezoelectric transducers not in resonance which reduces their effectivity considerably. For $\omega_M = v_L/\delta$ a maximum in the efficiency should occur (v_L is the longitudinal sound velocity). Since $\omega_M \approx 7 \cdot 10^{10} \text{ s}^{-1}$ for aluminum and $\approx 10^{12} \text{ s}^{-1}$ for silicon nitride, the laser envelope contains no Fourier components of such high frequencies. Hence this maximum remains unobservable at our experimental conditions. Therefore we are left with the explanation that the maximum originates from two competing processes: the increase of the efficiency of the thermoelastic effect because the ratio δ/λ increases with increasing frequency, and the decrease of the Fourier components due to the finite width of the laser pulse. This can be written in a more quantitative way:

$$S(\omega) = \frac{\omega^2 \delta^2}{\omega^2 \delta^2 + v_L^2} \cdot \beta \Theta_0(\omega) \cdot \frac{I}{\sqrt{\pi}} \exp(-\omega^2 \tau^2 / 4) d\omega \quad (2)$$

In this equation β is the thermal expansion coefficient and Θ_0 is the initial temperature increase at the surface ($\Theta_0 = P_0 \sqrt{\kappa/K\sqrt{\omega}}$). The second factor in Eq.(2) is the Fourier transform of the laser pulse envelope, whereas the first factor corresponds to the original expression derived by White for thermoelastic sound generation at unconstrained surfaces $1/\tau$. Inserting the proper parameters for silicon nitride, we obtain the dashed line shown in Fig. 3. It reproduces the maximum and the frequency spectrum at high frequencies quite reasonably. The low frequency part of the spectrum, however, varies theoretically as $\propto \sqrt{\omega}$ whereas the experiment yields rather $\propto \omega$. At present we do not have an explanation for this behavior.

It is straightforward to derive from Eq. (2) the frequency at which a maximum should occur. One obtains $\omega = 1/\tau$ independent of material parameters provided $\omega \ll v_L^2/2\kappa$. At least for the two materials examined, this could be verified experimentally. It should be noted that it is difficult to calculate the absolute magnitude of the strain curve versus frequency because $S(\omega)$ contains the absolute power density P_0 absorbed at the surface. Since we only could estimate this quantity, we can say at present that the experimental absolute magnitudes ($\approx \text{\AA}$ for $\approx 10 \text{ MW/cm}^2$ absorbed optical intensity) are roughly a factor of 5 smaller than the theoretical ones. We will discuss this point in a forthcoming publication in more detail /12/. It is obvious that a one-dimensional description leading to Eq. (2) can only explain the generation of longitudinal waves because shear waves are caused by lateral thermal expansion at the surface. Apparently, if the laser beam is not focused onto the surface, longitudinal waves are predominantly generated.

A new feature appears when the laser power is increased so that ablation of surface material sets in ($\approx 50 \text{ MW/cm}^2$). Then the strain levels become so large that second harmonic generation caused by lattice anharmonicity /13/ becomes noticeable. A typical strain curve versus frequency obtained under such conditions is shown in Fig. 4. At twice the frequency of the maximum in $S(\omega)$ a shoulder appears. Furthermore, lattice anharmonicity leads to a distant dependent build-up of the harmonic wave S_2 , because the fundamental strain wave $S_1(x)$ is attenuated by absorption as well as by the nonlinear process. We can explain this build-up quantitatively by solving two coupled differential equations for $S_1(x)$ and $S_2(x)$ which takes this into account /12/. The main parameters in these equations are c_3 and c_2 which are the appropriate third-order and second-order elastic constants, respectively.

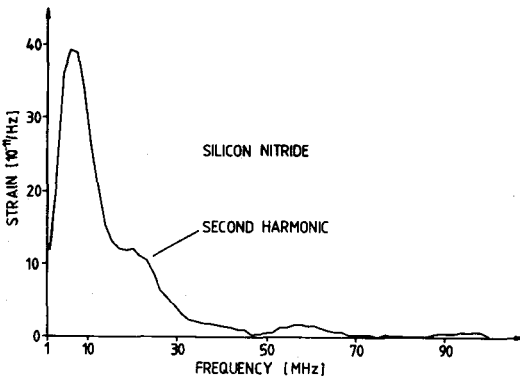


Fig.4: Frequency components of the strain pulse in silicon nitride at large optical intensities at which the longitudinal wave is enhanced by the recoil mechanism caused by ablation of surface material. A shoulder appears at twice the frequency of the maximum of $S_1(\omega)$. Lattice anharmonicity is at the origin of this effect.

Summarizing, we should like to point out that thermoelastic sound generation exhibits a pronounced frequency spectrum determined by the Fourier components of the laser pulse envelope, and by the frequency-dependent thermal penetration depth. Avoiding too high lateral thermal expansion at the surface, only longitudinal waves are generated. At least in the overall behavior their frequency spectrum and absolute magnitude can be explained by a simple one-dimensional theoretical description.

References

- /1/ White, R.M., J. Appl. Phys. 34, 3559 (1963).
- /2/ Carome, E.F., Clark, N.A., and Moeller, C.E., Appl. Phys. Lett. 4, 95 (1964).
- /3/ Cachier, G., J. Acoust. Soc. Am. 49, 947 (1971).
- /4/ Brienza, M.J. and de Maria, A.J., Appl. Phys. Lett. 11, 44 (1967).

- /5/ von Gutfeld, R.J. and Melcher, R.L., Appl. Phys. Lett. 30, 257 (1977).
- /6/ Hu, C.L., J. Acoust. Soc. Am. 46, 728 (1969).
- /7/ Sigrist, M.W. and Kneubühl, F.L., J. Acoust. Soc. Am. 64, 1652 (1978).
- /8/ Lyamshev, L.M. and Sedov, L.V., Sov. Phys.-Acoust. 27, 4 (1981) and references contained therein.
- /9/ Emmony, D.C., Geerken T., and Klein-Baltink, H., J. Acoust. Soc. Am. 73, 220 (1983).
- /10/ Hutchins, D.A., Dewhurst, R.J., and Palmer, S.B., J. Acoust. Soc. Am. 70, 1362 (1980).
- /11/ see for example Aindow, A.M., Dewhurst, R.J., Hutchins, D.A. and Palmer, S.B. J. Acoust. Soc. Am. 69, 449 (1981).
- /12/ Arnold, W. and Betz, B., in preparation
- /13/ Breazeale, M.A. and Ford, J., J. Appl. Phys. 36, 3486 (1965).